Journal Pre-proofs

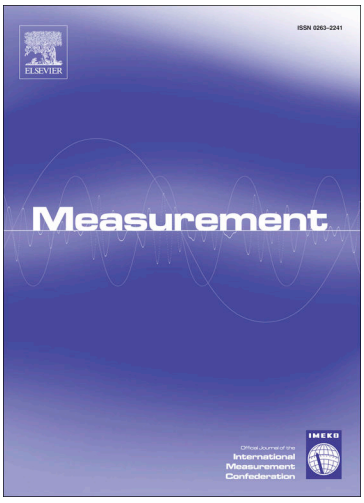

Application of the Combined Teager-Kaiser Envelope for bearing fault diagnosis

A. Galezia, K. Gryllias

PII: S0263-2241(21)00673-4
DOI: https://doi.org/10.1016/j.measurement.2021.109710
Reference: MEASUR 109710

To appear in: *Measurement*

Received Date: 31 December 2020
Revised Date: 20 May 2021
Accepted Date: 3 June 2021

Please cite this article as: A. Galezia, K. Gryllias, Application of the Combined Teager-Kaiser Envelope for bearing fault diagnosis, *Measurement* (2021), doi: https://doi.org/10.1016/j.measurement.2021.109710

Application of the Combined Teager-Kaiser Envelope for bearing fault diagnosis

A. Galezia [1,2,3], **K. Gryllias** [2,3]
[1] Faculty of Automotive and Construction Machinery Engineering, Warsaw University of Technology
[2] Department of Mechanical Engineering, KU Leuven
[3] Dynamics of Mechanical and Mechatronic Systems, Flanders Make
e-mail: **adam.galezia@kuleuven.be**

Highlights

- The paper presents multiband approach for bearing failure detection.
- The signal processing applies the demodulation based on Teager-Kaiser energy operator.
- Experimental investigation confirmed potential of the method for detection of bearing failures.

Abstract

Rolling element bearings are among the most important components of rotating machinery, being the interface between the stationary and the rotating parts. Bearing failures might cause accidents and unexpected machine breakdown. Therefore, there is an important need for novel condition monitoring techniques focusing towards early detection and accurate identification of emerging faults. The key aim of this paper is the proposal of the concept of Multiband Demodulation Analysis (MDA), performed using a bank of bandpass Gabor filters combined with the Teager-Kaiser Energy Separation Algorithm (ESA) for condition monitoring of rolling element bearings. The demodulation takes place in multiple frequency bands, following a multiband analysis scheme, in order to isolate the strongest modulation components in each band. Finally, a maximum average energy tracking process over the various frequency bands is used to yield short-time measurements of the multiband signal modulation energy and the demodulated instant amplitude and frequency. The method is applied, tested and evaluated on vibration signals, captured on two test rigs and its performance is compared with a state of the art diagnostic approaches, the Kurtogram and the empirical mode decomposition, achieving promising results.

Keywords: Condition Monitoring, Bearing diagnostics, Teager-Kaiser Energy Operator, Envelope Analysis, Multiband Analysis

1 Introduction

The ever emerging need for safe operation and high reliability of rotating machines enforces the constant development of signal processing and analysis techniques for condition monitoring. The research work aims at the extraction of diagnostic features/indicators which are strongly related to the component's technical state. Rolling element bearings are among the most common and critical components of rotating machines.

A failure of a bearing can lead to sudden and unexpected machinery breakdown as well as to human casualties and environmental pollution. Therefore the main task of condition monitoring is to identify the actual degree of degradation as this knowledge allows to undertake suitable maintenance actions.

Although a plethora of methods of condition monitoring of bearings have been proposed during the last decade, the correct and accurate identification of the technical state is still a challenging task. In order to extract useful diagnostic features from time signals, it is required to overcome a number of challenges such as: poor Signal-to-Noise Ratio (SNR), interference of other diagnostic signals sources such as gears in gearboxes etc. Additionally, the state of fault development might cause that the diagnostic signal does not contain a clear fault pattern (Fig. 1). Therefore, novel condition monitoring techniques, based on the time domain, the frequency domain, the time-frequency domain and the cyclostationary domain are constantly proposed ([1], [2], [3], [4], [5], [6], [7]) in an effort to achieve early and accurate fault detection and diagnosis. In industrial applications, diagnostics of bearings using vibration signals gained high popularity, mainly due to acceptable cost and high reliability of vibration sensors, ability to locate sensor close to source of signal. However, attempts to use acoustic signals are also known [8], [9]. The application scope of acoustic condition monitoring is strongly dependent on the level and character of background noise, sometimes causing this approach difficult to implement in plant practice. Another possible drawback of application of acoustic signals in condition monitoring is need of use of sophisticated software [10], [11], and/or hardware [12] tools for separation and identification of source. A main advantage of acoustic condition monitoring is ability to record signals in distance from the source what can be useful if access to machine is difficult or hazardous. Because data sets used for validation of presented method were recorded using acceleration sensors, the presented signal processing approach was implemented on vibration signals.

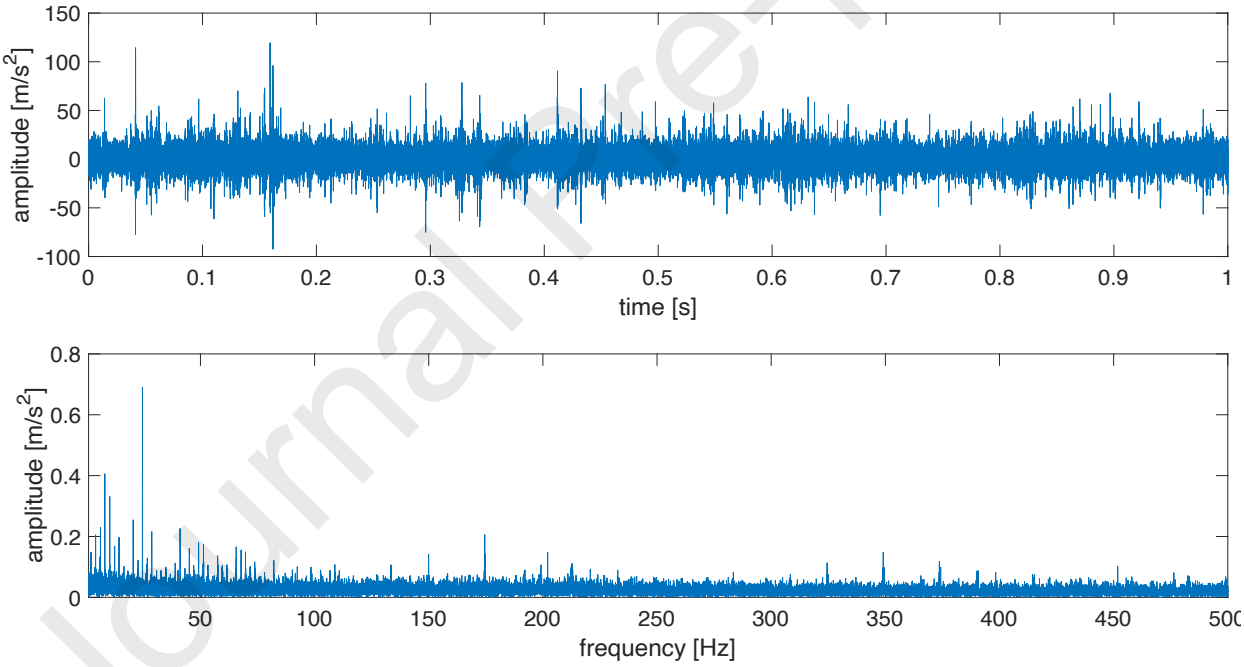

Fig. 1. The time waveform and the corresponding envelope spectrum of a bearing signal with unclear outer race fault pattern obtained during laboratory tests (further described in section 3.1).

A wide variety of condition monitoring methods dedicated to rolling element bearings have been proposed, such as tools based on statistical parameters e.g. kurtosis, crest factor [13] or XSK [14]. Those parameters are usually obtained from the raw signal [15] or its envelope [16]. Another category consists of methods based on the frequency-domain. In this case, usually a spectrum is analyzed in order to detect the existence of the characteristic bearing fault frequencies. Among others, the most popular method is the envelope analysis. In the first step, the vibration signal is band-pass filtered usually around a resonance frequency of the bearing-housing system. An envelope of the filtered signal is obtained by a demodulation process. Most often, the demodulation is performed using the Hilbert transform.

The optimal filter band for envelope analysis, should be characterized by high Signal-to-Noise ratio. In such a band, the fault harmonics should be easily visible [16], [17]. In practice, the band is selected based on engineering experience or using tools such as the Fast Kurtogram (FK) [18]. FK selects the band with the maximum kurtosis level. Moreover Autogram [19] is also based on the maximum kurtosis but is obtained based on the unbiased autocorrelation of the squared envelope of the demodulated signals. The band of the autocorrelated squared envelope with the highest Kurtosis is selected as the optimal one for demodulation. Furthermore the last years a number of researchers is also focusing on the application of machine learning methods for fault detection and identification [20], [21].

In the classical envelope analysis approach, fault detection is performed analyzing only a single band. A novel approach assumes that additional information could be collected if the demodulation is realized in more than one bands simultaneously. This idea has been first applied in speech processing and very recently in bearing diagnostics under different concepts, e.g. the Combined Squared Envelope Spectrum (CSES) [19], the Combined Improved Envelope Spectrum (CIES) [22] etc.

In this paper the concept of the Multiband Demodulation Analysis (MDA), based on the application of a bank of bandpass Gabor filters [23] and the application of the Teager-Kaiser Energy Separation Algorithm (ESA) [24], is proposed, tested and evaluated for fault detection of rolling element bearings. The demodulation takes place in multiple frequency bands, following a multiband analysis scheme [25], to isolate the strongest modulation components in each band. The method is firstly applied and evaluated on two sets of vibration signals from bearings with different faults working under different operation conditions and then is compared with the Kurtogram, which is considered as a state of the art technique, as well as single intrinsic mode function (IMF) extracted using empirical mode decomposition (EMD) algorithm.

The rest of the paper is organized as follows. First the proposed methodology, including the Teager-Kaiser Energy Operator and the Combined Teager-Kaiser Envelope, is presented in Section 2. Moreover the methodology is applied, tested and evaluated on two datasets (the first one is obtained from the Institute of Applied Mechanics of Poznan University of Technology and the second from the Department of Mechanical and Aerospace Engineering of Politecnico di Torino) and the results are presented and compared with the results obtained by the Fast Kurtogram in Section 3. The paper closes with the conclusion and a short discussion on the advantages and the drawbacks of the Combined Teager-Kaiser Envelope as well as with ideas for further development.

2 Description of the proposed methodology

In this paper a novel approach, which aims to enhance the diagnostic information by applying the Teager-Kaiser Energy Operator (TKEO), is proposed in order to identify the most informative frequency bands of the analysed signal. The Combined Teager-Kaiser Envelope ($C_{TK}Env$), which will be presented in the next subsection, is a novel multiband approach where the raw signal is first divided into a number of bands in order to extract the bearing diagnostic information and then it is weighted summed up, creating the $C_{TK}Env$. The proposed approach uses the TKEO in order to obtain the instantaneous value of the energy of the considered signal and to perform the demodulation process. In the following subsections the signal processing and signal analysis concepts are analytically presented.

2.1 Rolling element bearing fault characteristic frequencies

Most popular targeted approaches, dedicated to condition monitoring of rolling element bearings, use features estimated in the time or frequency domain. The latter approach is mainly based on the identification of the bearing fault characteristic frequencies: BPFO (1), BPFI (2), BSF (3) and FTF (4).

$$\mathrm{BPFO} = 60 \cdot \omega_{rot} \frac{N}{2}\left(1 - \frac{d}{D_p}\cos(\beta)\right) \tag{1}$$

$$\mathrm{BPFI} = 60 \cdot \omega_{rot} \frac{N}{2}\left(1 + \frac{d}{D_p}\cos(\beta)\right) \tag{2}$$

$$\mathrm{BSF} = 60 \cdot \omega_{rot} \frac{D_P}{d}\left(1 - \left(\frac{d}{D_P}\cos(\beta)\right)^2\right) \tag{3}$$

$$\mathrm{FTF} = \frac{60 \cdot \omega_{rot}}{2}\left(1 - \frac{d}{D_P}\cos(\beta)\right) \tag{4}$$

where:
ω_{rot} – the rotation speed [Hz], N – the number of rolling elements, d – the rolling element diameter [mm], D_P – the pitch diameter [mm], β – the contact angle [rad].

The above equations (1-4) provide a nominal value and are not strict for real operation conditions due to e.g. variations of the contact angle and slip which may lead to a slightly different true fault frequencies. The variation of the contact angle might be caused by misalignment, thermal growth or other factors. An additional problem might be the unknown true rotation speed.

2.2 The Teager-Kaiser Energy Operator

The Teager-Kaiser Energy Operator (TKEO) is a differential operator presented by Kaiser in 1990 [24]. The properties of the operator have been discussed extensively in [26], [27] and [28]. The TKEO itself and the TKEO based measures have been already effectively applied to tasks including demodulation [29], [30] signal processing and diagnostics of gears and bearings [3], [31], [32], [33]. The energy operator also proved to be sensitive to impulses [34] which could be generated by faults. The authors decided to direct their attention to the application of the Teager-Kaiser Energy Operator mainly because changes in both amplitude and frequency of the analysed signal will be reflected in the estimated energy. The TKEO is sensitive to transient changes occurring in signals [35] resulting from emerging faults. Additionally, it is easy to implement and has demodulation capabilities [36] suitable for signals with short duration. Limiting the signals to the frequency band of interest improves the quality of the energy estimation using the TKEO.

The TKEO of a time domain signal can be defined as (5):

$$\Psi(x(t)) = \dot{x}^2(t) - x(t)\ddot{x}(t) \tag{5}$$

while for discrete signals (1) can be re-written as (6):

$$\Psi_d(x_n) = {x_n}^2 - x_{n-1}x_{n+1} \tag{6}$$

For a harmonic signal $x(t) = A\cos(\omega t)$, the instantaneous value of the Teager-Kaiser energy $E_{TK}(t)$ depends on the instantaneous value of the squared amplitude and the squared frequency (7) of the signal [24].

$$E_{TK}(t) = \Psi(x(t)) = A^2\omega^2 \tag{7}$$

The signal demodulation process based on the TKEO has been discussed in [37] and is given by (8) and (9).

$$\omega^2(t) = \frac{E_{TK}(\dot{x}(t))}{E_{TK}(x(t))} \tag{8}$$

$$A^2(t) = \frac{E_{TK}(x(t))^2}{E_{TK}(\dot{x}(t))} \tag{9}$$

For discrete signals, several demodulation algorithms exist [38], however the most common one is the DESA-2 algorithm presented in [37]. This algorithm is using the approximation of the first derivative with a symmetric 2 samples difference (10), (11).

$$\Omega_n \approx \frac{1}{2}\arccos\left[1 - \frac{\Psi_d(x_{n+1} - x_{n-1})}{2\Psi_d(x_n)}\right] \tag{10}$$

$$Env \approx \frac{2\Psi_d(x_n)}{\sqrt{\Psi_d(x_{n+1} - x_{n-1})}} \tag{11}$$

where: Ω_n is a signal of the instantaneous frequency consisting of discrete samples and Env is the envelope signal in the discrete-time domain.

The approach discussed in the next subsection uses the TKEO in two ways: on one hand to calculate the energy of a signal and on the other hand to perform demodulation in order to obtain its envelope.

2.3 The Gabor filter

A vibration signal, recorded on an operating bearing, is band-pass filtered by a set of Gabor filters (13).

$$H(\omega) = \frac{\sqrt{\pi}}{2\alpha}\left[exp\left(-\frac{(\omega-\omega_c)^2}{4\alpha^3}\right)exp\left(-\frac{(\omega+\omega_c)^2}{4\alpha^3}\right)\right] \quad (13)$$

where: $H(\omega)$ is the frequency response of a Gabor filter, ω_c is the centre frequency, α is the filter's root mean square (RMS) bandwidth.

The Gabor filter was chosen due to its good time and frequency resolutions [39]. Each filter is defined by its centre frequency ω_c and a -3dB filter width. The centre frequencies of all filters, with same filters' width, allow the complete set of filters to cover the entire frequency range of the analysed signal (6) (Fig. 2). As described in section 3, the filter width was chosen for each validation case separately to cover at least the two first harmonics of $BPFI$ with sidebands.

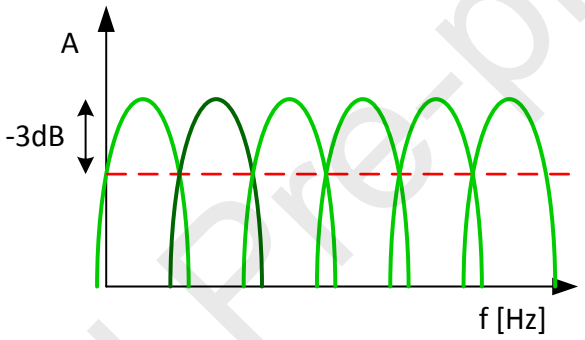

Fig. 2. Scheme of Gabor filters covering the entire signal band.

2.4 The Combined Teager-Kaiser Envelope

The scheme (Fig. 3) presents the concept of the proposed signal processing leading to the Combined Teager-Kaiser Envelope $C_{TK}Env$.

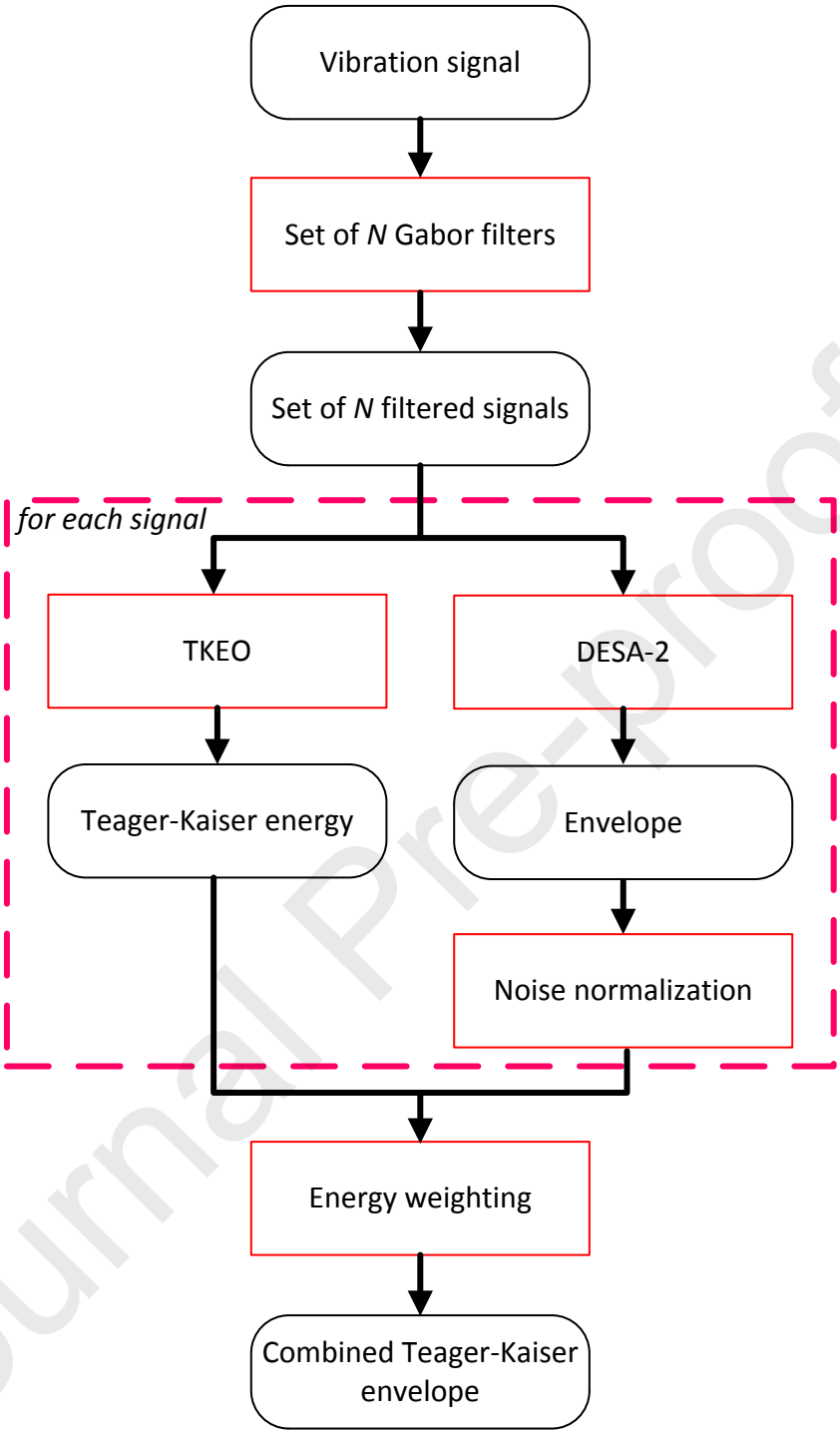

Fig. 3. The flowchart of the proposed methodology for the extraction of the Combined Teager-Kaiser Envelope

The number of the frequency bands analysed in this approach depends on the selected -3dB filter width. It must be remembered that this parameter defines the number of the harmonics of the fault frequencies observed in the envelope spectrum. As a result of the filtration process, a set of N bandpass filtered time domain signals is obtained. Next, the DESA-2 algorithm is used to perform demodulation of the filtered signals resulting in a number of envelopes (11). The envelopes are normalized with respect to the noise components (14), to supress the influence of the bands which may contain weak fault characteristic peaks compared to the surrounding noise components.

$$\widehat{Env}_i = \frac{Env_i}{\frac{1}{2\alpha}(X - X_{failure})} \tag{14}$$

where: α is the filter's rms bandwidth, X is the spectrum of the filtered signal, $X_{failure}$ is the spectrum containing the fault characteristic components.

In the framework of the procedure, the Teager-Kaiser energy operator is also used to calculate the overall energy E_i of the i-th filtered signal, as a sum of the instantaneous values of the signal's TK energy. This overall energy is used as a weighting factor in the Combined Teager-Kaiser Envelope (15).

The proposed multiband approach uses information from different frequency bands of the signal in order to obtain the Combined Teager-Kaiser Envelope ($C_{TK}Env$) (15) as a sum of all the weighted noise normalized envelopes.

$$C_{TK}Env = \sum_{i=1}^{N} \frac{E_i}{E} \widehat{Env}_i \tag{15}$$

where: $C_{TK}Env$ is the Combined Teager-Kaiser Envelope, E_i is the Teager-Kaiser energy of the signal filtered by the i-th Gabor filter, N is the number of the Gabor filters, $\widehat{Env}_i$ in the envelope of the signal filtered by the i-th Gabor filter (11).

Due to the fact that in the classical approach the initial choice of the single band might not be optimal making more difficult the fault diagnosis, the presented $C_{TK}Env$ takes also into account information from other frequency bands. Due to the weighting, based on the contribution of each band into the signal's overall energy, the influence of the bands containing mainly low amplitude noise is supressed.

To investigate the applicability of the Combined Teager-Kaiser Envelope its spectrum will be compared with the envelope spectrum from the optimal band selected by the Fast Kurtogram, where the kurtosis is maximised as well as with spectrum of most-fault informative IMF obtained by EMD [40]. The application of the TKEO and the Gabor filters allows to take advantage of both tools: the estimated energy of the signal carries information on a fault regardless it is manifested as amplitude or frequency variations and good time/frequency resolution trade off allows for the extraction of good quality information from both domains.

2.5 The Noise Contribution Ratio indicator

In order to evaluate the effectiveness of the proposed methodology $C_{TK}Env$, Fast Kurtogram [18] and EMD [41] were chosen as the reference methods. Kurtogram is a map presenting the distribution of spectral kurtosis in frequency bands of the analysed signal. Kurtosis indicates the peakiness of the signal and it is used often for bearing fault detection. The Kurtogram is a state of the art method used in condition monitoring of rolling element bearings. The EMD decomposes analysed signal $x(t)$ into set of intrinsic mode functions $imf_i(t)$ and a residual $r(t)$ (16):

$$x(t) = \sum_{i=1}^{N} imf_i(t) + r(t) \tag{16}$$

The EMD is a popular tool used for fault diagnosis [41], [42], [43] however it also can be applied for denoising and detrending of signals [44], [45], [46]. Based on method described in [47], which applied Pearson correlation coefficient of each IMF and the empirically determined local mean of the original signal, IMF's of analysed vibration signal were divided in to three classes: "noise-only" IMF's, "signal-only" IMF's and "trend-only" IMF's (Fig. 4). The IMF's with low indices and low value of correlation coefficient contained mostly noise while IMF's with high indices and low value of correlation coefficient contain trend components. Classification of IMF's to particular groups depends from defined threshold. The main goal was to extract such IMF which would contain signatures associated with bearing faults. The experimental analysis revealed, that for further described test cases, most informative was "signal-only" IMF with lowest index, therefore spectrum of such IMF was chosen for comparison with the spectrum of Combined Teager-Kaiser Envelope. Due to the fact that test-rigs, described in following sections, did not contain additional power transmission components such as gearboxes, maximum number of calculated IMF was 10. Increasing number of calculated IMFs did not improved the readability of spectral fault patterns.

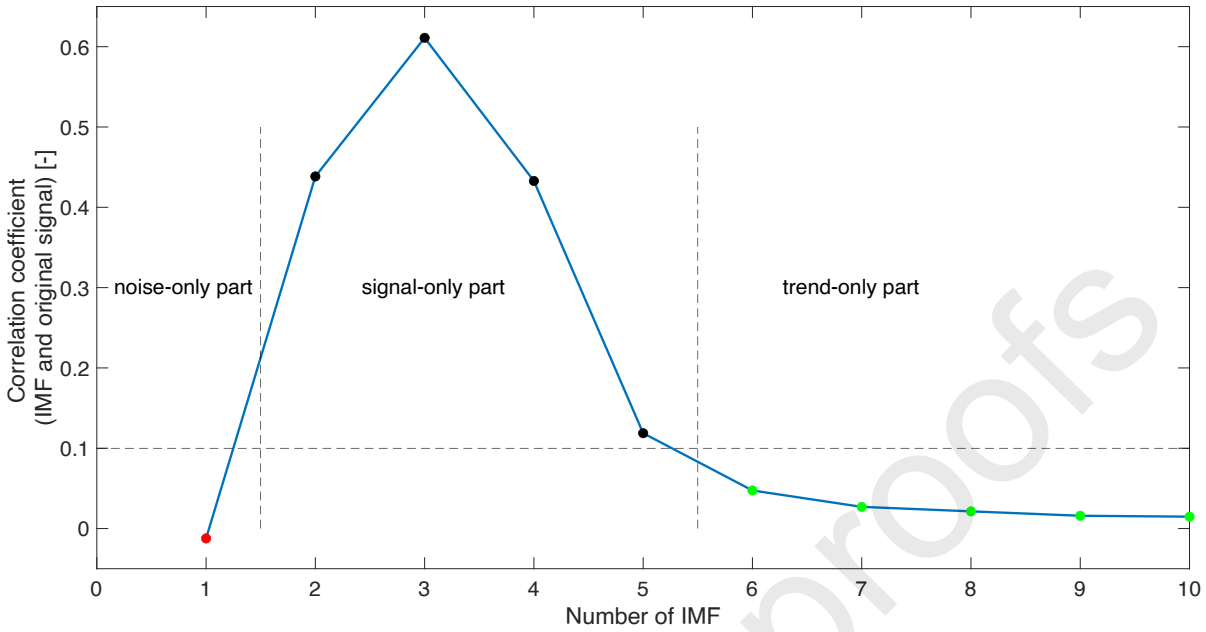

Fig. 4. Exemplary assigning of IMF to various parts of signal for one of considered test cases.

To quantify the contribution of the noise components in the spectrum, for all approaches, the Noise Contribution Ratio indicator $NCR_{C_{TK}Env}$ (17) is used. For the frequency range of interest, labelled as $freqs$, the $NCR_{C_{TK}Env}$ compares the total sum of amplitudes of the normalized envelope spectra F_{norm} of the most informative part of the signal obtained using both: the reference method, i.e. Kurtogram and EMD, x_{ref} and the Combined Teager-Kaiser Enveope $C_{TK}Env$ respectively. The frequency ranges of interest, used for comparison of $C_{TK}Env$ and the reference methods, were set independently for each fault type under consideration based on subjective decision. It was decided to look at the region around the fault frequencies (BPFI, BPFO, BSF) but excluding potential modulation peaks. The reason to limit the region of comparison in such way was caused by the need to mitigate the method dependent influence of the variable heights of side-peaks. For example, for the inner race fault the frequency range of interest was defined as: $freqs = (BPFI - \omega_{rot}, BPFI + \omega_{rot})$, i.e. covering the band around the carrier frequency excluding the modulation peaks. A similar concept was used for the rolling element fault, where $freqs = (BSF - FTF, BSF + FTF)$. On the other hand, as the outer race fault characteristic frequency is not accompanied by modulation peaks, for this type of fault the comparison frequency range was $freqs = (BPFO - 0.9\,BPFO, BPFO + 1.1\,BPFO)$. The $NCR_{C_{TK}Env}$ values higher than 1 indicate that the spectrum of the $C_{TK}Env$ contains lower contribution of noise components comparing to the spectrum of the band chosen using Kurtogram or spectrum of chosen IMF.

$$NCR_{C_{TK}Env} = \sum_{(freqs)} |F_{norm}(x_{ref})| \Big/ \sum_{(freqs)} |F_{norm}(C_{TK}Env)| \tag{17}$$

3 The Combined Teager-Kaiser Envelope for condition monitoring

The Combined Teager-Kaiser Envelope for condition monitoring of rolling element bearings is applied, tested and evaluated using two data sets: the first one contains signals for different faults of bearings operating under constant speed and load; the second one contains data from bearings with faulty roller and operating under variable speed and load conditions. The performed tests aim to identify the advantages and

the disadvantages of the proposed method as well as to compare the obtained results with the ones acquired using the Fast Kurtogram and EMD.

3.1 Validation Case 1 – Dataset of Poznan University of Technology – Steady operating conditions

The data set consists of vibration signals recorded for variable faults of bearings working under the same operational conditions.

3.1.1 Case 1 dataset description

The measurements were performed on a test stand of the Institute of Applied Mechanics of Poznan University of Technology in Poland (Fig. 5) [3]. The test bearing is a tapered roller bearing CBK-171. The data set consists of vibration signals from 9 bearings in different technical state (Table 1). The technical states are considered as artificially introduced faults, located on the rolling element, the inner or the outer race. The faults were created either by electroerosion or by sandblasting. The faults differ in size and mean depth. Photos of the selected faults indicated by the defect code are presented in Figure 6. The yellow arrows and the red lines indicate the location and the size of the presented faults. It should be highlighted that at the photo of the undamaged bearing two shadows are visible.

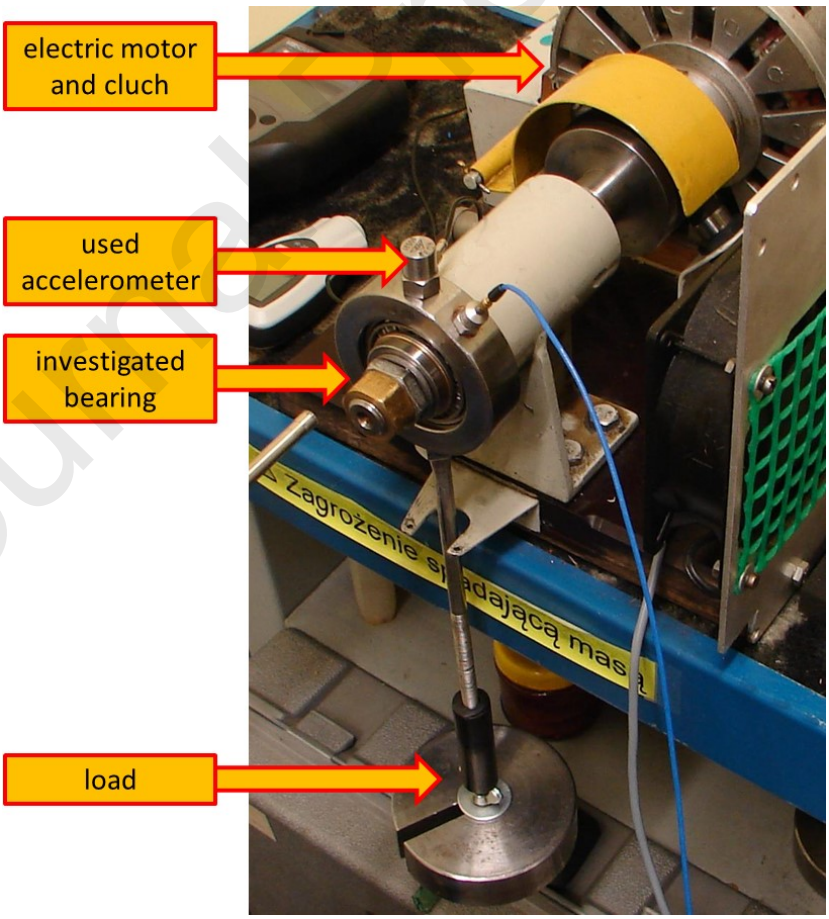

Fig. 5. The test rig of Poznan University of Technology

Table 1: Bearings description [3]

Defect code	Bearing code	Faulty element	Damage type	Defect size	Defect width [mm]	Defect depth [μm]
UD	N02	undamaged	–	–	–	–
IR(EL)	N00	inner race	Electroerosion	local	0,5	Na
RE(EL)	N19	rolling element	Electroerosion	local	1	Na
OR(EL)	N14	outer race	Electroerosion	local	2	approx. 85
OR(EW)	N17	outer race	Electroerosion	wide	11	approx. 50
OR(EF)	N03	outer race	Electroerosion	extensive	whole race	approx. 50
OR(SL)	N12	outer race	Sandblasting	local	3	approx. 12
OR(SW)	N01	outer race	Sandblasting	wide	11	approx. 12
OR(SF)	N16	outer race	Sandblasting	extensive	whole race	approx. 13

The tests were performed under constant operational conditions: axial bearing load F_A = 55 [N]; radial (vertical) gravitational load applied by a mass m equal to 1545 [g]; F_V = 15,16 [N]; rotating speed 1450 [rpm]. The test stand was equipped with a tachometer, which allowed to control the rotation speed. In the presented study, the vertical vibrations recorded on the top of the bearing housing are used. The signals were recorded with sampling frequency equal to 97660 [Hz]. The frequency range of the analysed signals was covered by 55 Gabor filters with a bandwidth equal to 900 Hz.

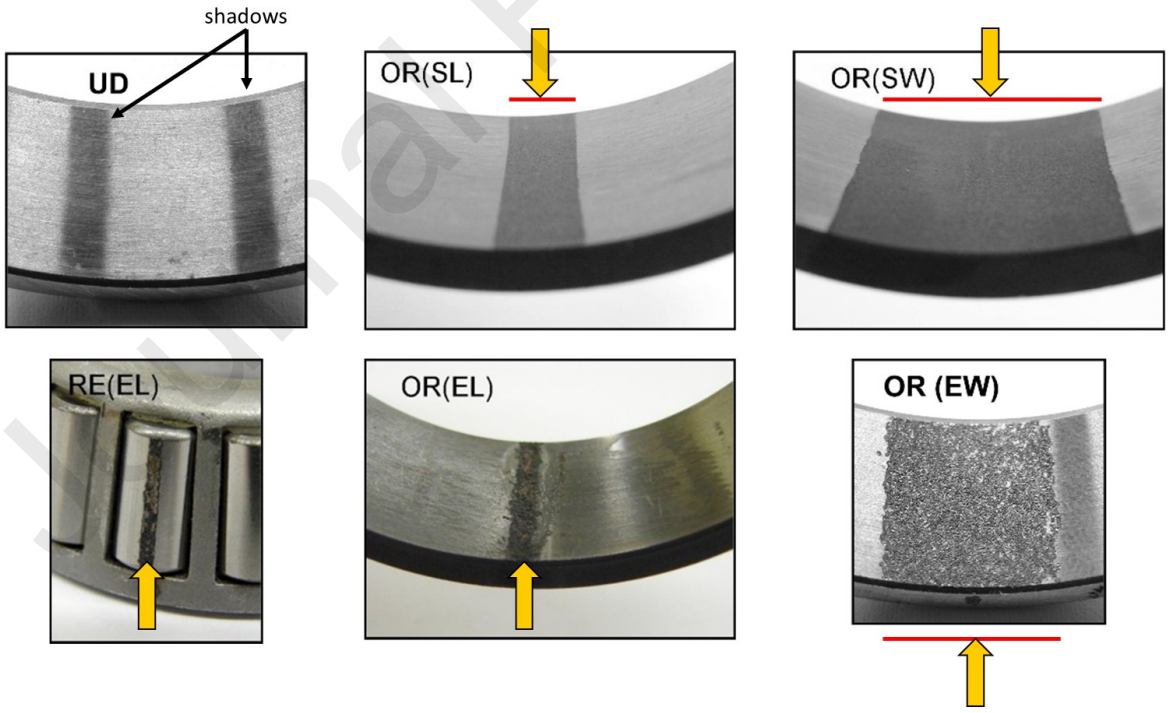

Fig. 6. Selected faults of the tested bearings.

3.1.2 Application of the $C_{TK}Env$ to Case 1 data

The nominal rotation speed ω_{rot}, for all tested CBK-171 bearings, was 24.16 rotations per second. The nominal fault frequencies are presented in table 2.

Table 2: Nominal fault frequencies for the CBK-171 bearing

Rotation speed ω_{rot} (Hz)	FTF (Hz)	BSF (Hz)	2x BSF (Hz)	BPFO (Hz)	BPFI (Hz)
24.16	10.13	70.61	141.22	172.24	238.59

The vibration signals from each measurement, described in Table 1, are analysed using the presented approach. For each measurement, the actual rotation speed was determined based on the tachometer signal and it was approximately 2% higher from the nominal value, ranging from 24.54 to 24.63 Hz among the measurements. The following subsections discuss, for some selected faults, the results obtained with the Combined Teager-Kaiser Envelope and the reference methods.

3.1.3 Bearing IR(EL)

First the Combined Teager-Kaiser Envelope spectrum and the envelope spectrum based on the Kurtogram are estimated for a bearing, with an inner race fault caused by electroerosion, and are presented in Figure 7. The Kurtogram identified the most informative band located around the center frequency $fc = 42726{,}25$ [Hz] with a bandwidth $bw = 12207{,}5$ [Hz]. Figure 8 presents comparison between spectrum of IMF extracted using EMD method and the spectrum of the $C_{TK}Env$.

The presented spectra are normalized with respect to the peak in the frequency of interest, i.e. the BPFI in this case. It can be seen that the Combined Teager-Kaiser Envelope presents a lower level of noise components and therefore a number of frequency components in the $C_{TK}Env$ have lower amplitudes compared to the envelope spectrum obtained using the reference methods. In the considered case, the frequency range of interest was $freqs = (BPFI - \omega_{rot}, BPFI + \omega_{rot})$. For the bearing IR(EL) the $NCR_{C_{TK}Env}$ is equal to 1.23 in case of Kurtogram and 1.07 while comparing with IMF. This indicates that spectrum of the extracted intrinsic mode was less noisy than the spectrum obtained using Kutogram method. The $C_{TK}Env$ for the considered measurement with the indicated calculated characteristic fault frequencies is presented in Figure 9. The classical inner race fault pattern (a carrier and modulation peaks) is well indicated by the star symbols.

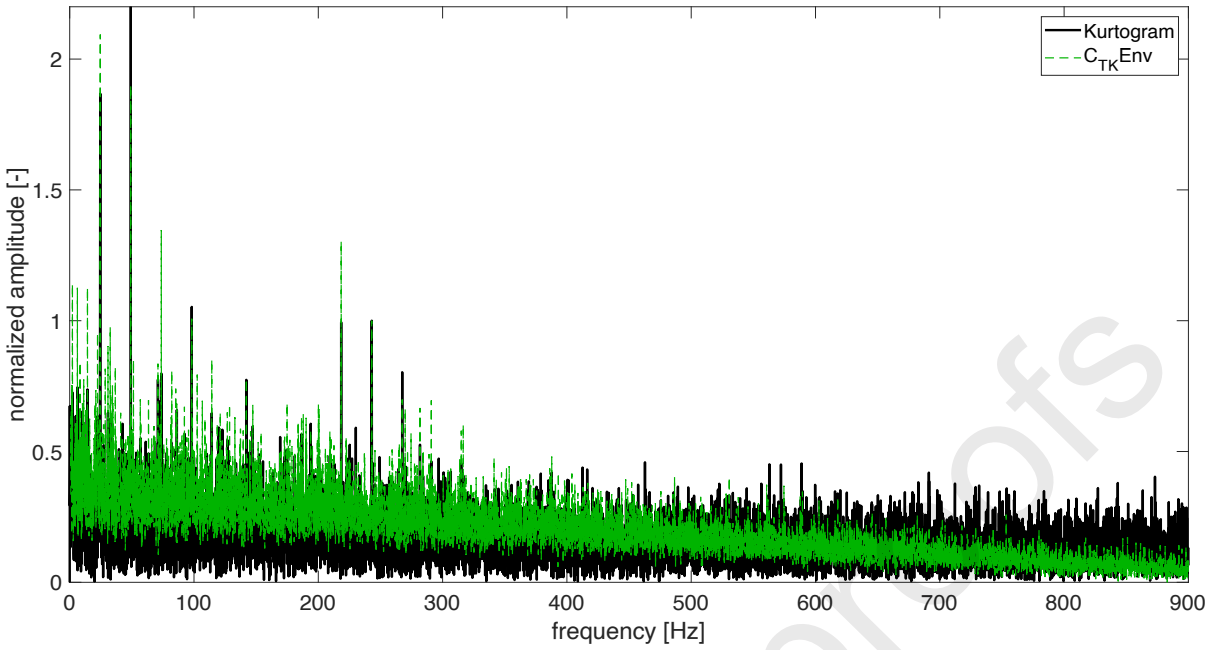

Fig. 7. Bearing IR(EL) - comparison of the normalized $C_{TK}Env$ (green) and the normalized envelope spectrum obtained from the Kurtogram (black).

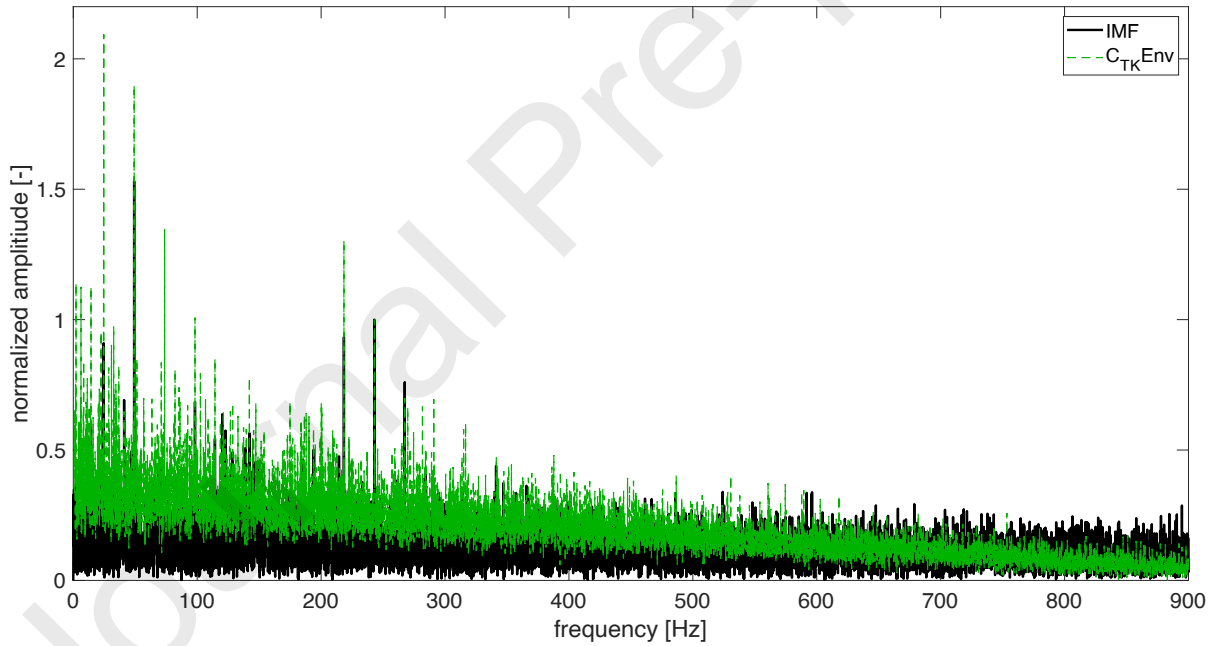

Fig. 8. Bearing IR(EL) - comparison of the normalized $C_{TK}Env$ (green) and the normalized envelope spectrum obtained from the IMF (black).

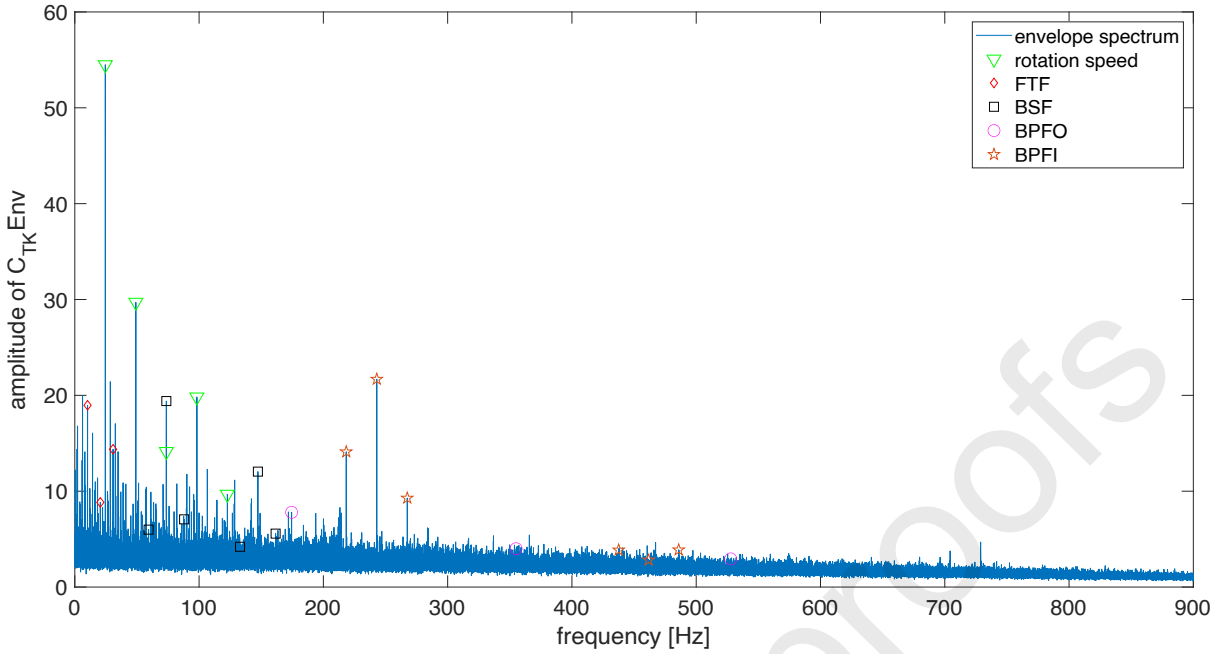

Fig. 9. Bearing IR(EL) - the $C_{TK}Env$ and the inner race fault frequency pattern indicated by the star symbol.

3.1.4 Bearing OR(EW)

The fault of the outer race causes the existence of peaks at the BPFO frequency and its higher harmonics. For the considered case of wide width of electroerosion fault, the normalized spectrum, with respect to BPFO, obtained with the Combined Teager-Kaiser Envelope contains lower noise components (Figure 10 and 11) and the fault frequencies of interest are enhanced. The $NCR_{C_{TK}Env}$ indicator (17) was calculated for the frequency band ranging from $BPFO - 0.9\,BPFO$ to $BPFO + 1.1\,BPFO$ and was equal to 1.18 comparing with results obtained using Kurtogram and 1.03 for IMF. The Kurtogram identified the most informative band to be the same as in IR(EL) case ($fc = 42726{,}25$ [Hz], $bw = 12207{,}5$ [Hz]).

The $C_{TK}Env$ for the OR(EW) bearing is presented in Figure 12. The circles indicate the calculated first 3 harmonics of the outer race fault frequency which are well visible in the spectrum. The applied approach allowed to highlight the characteristic fault components, allowing for the correct fault identification.

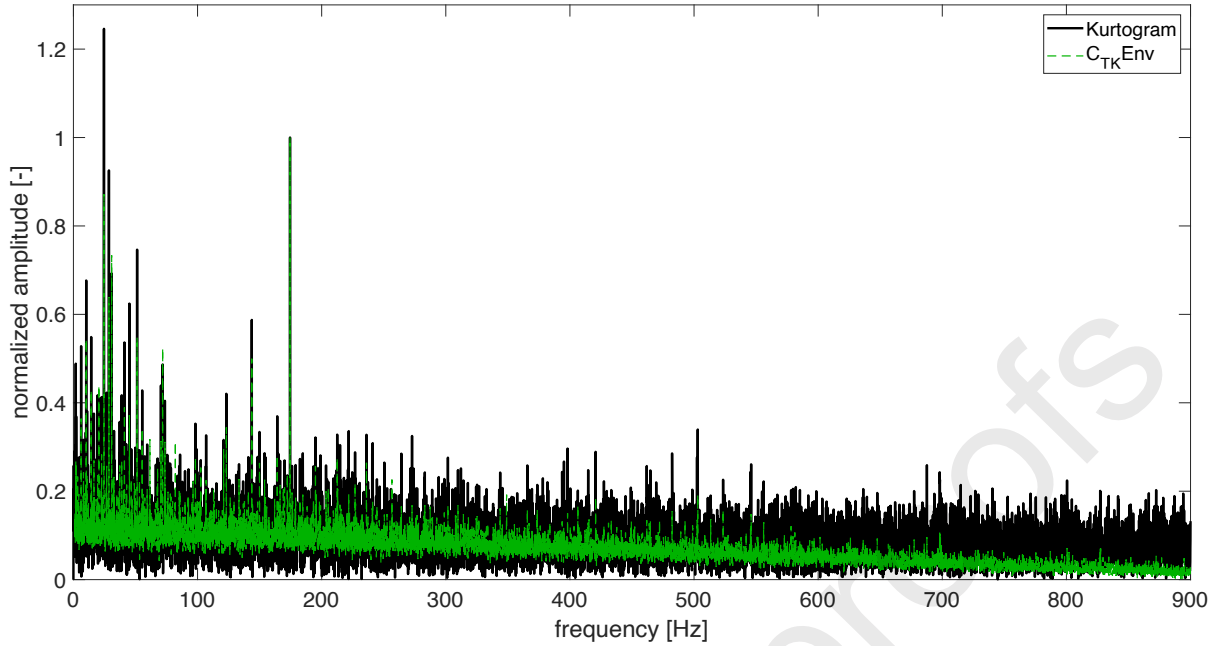

Fig. 10. Bearing OR(EW) – comparison of the normalized $C_{TK}Env$ (green) and the normalized envelope spectrum obtained from the kurtogram (black).

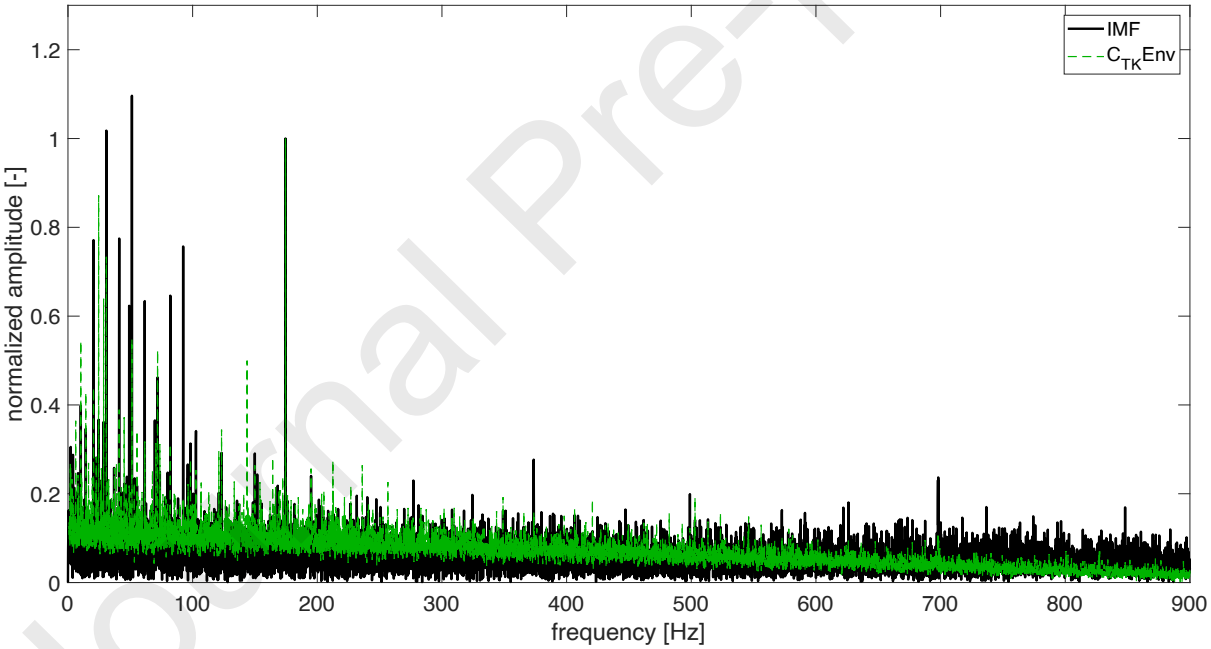

Fig. 11. Bearing OR(EW) – comparison of the normalized $C_{TK}Env$ (green) and the normalized envelope spectrum obtained from the IMF (black).

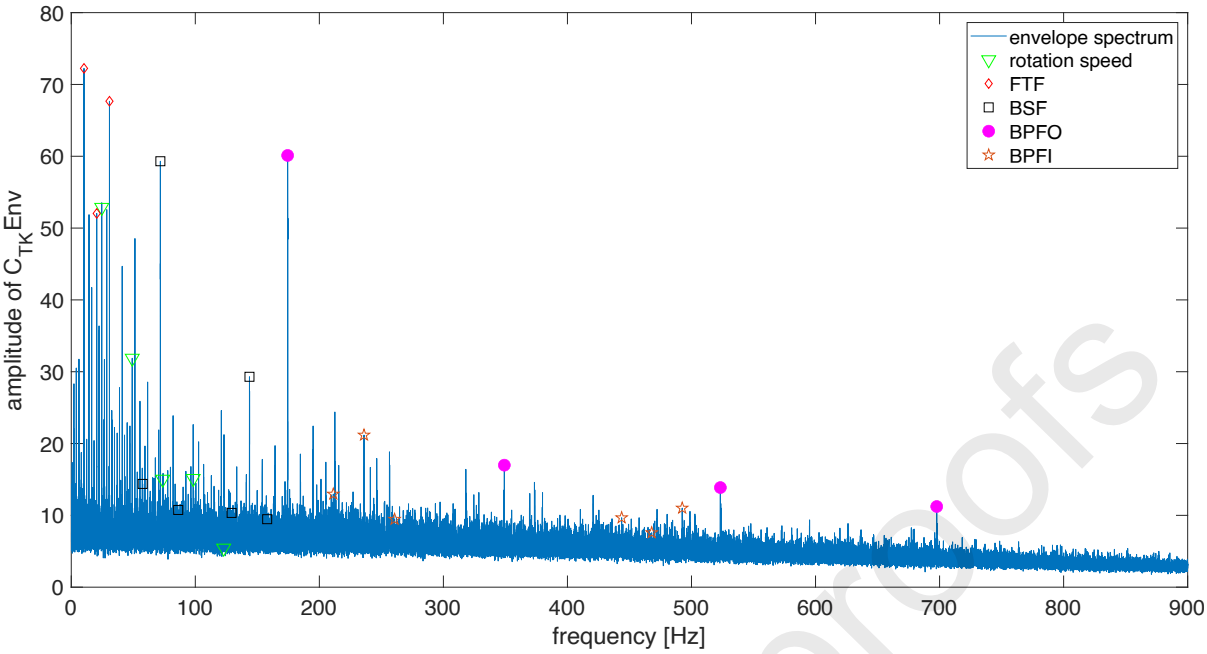

Fig. 12. Bearing OR(EW) - the $C_{TK}Env$ and the outer race fault frequency pattern indicated by the circle symbol.

Similar results have been obtained for the majority of the investigated measurements from this test case, leading to a general reduction of the contribution of the noise components with an amplification of the fault characteristic frequencies.

3.1.5 Bearing OR(SF)

In the considered set of data, the vibration signals recorded for outer race faults covering the complete circumference, i.e. OR(SF) and OR(EF), were analyzed with the presented $C_{TK}Env$ approach but reveal no classical pattern (Fig. 13). The severity of the fault excited a wide range of fault characteristic frequencies. Both the Combined Teager-Kaiser Envelope and the Kurtogram ($fc = 44760{,}83$ [Hz], $bw = 8138{,}33$ [Hz]) give similar results with slightly lower noise in the second approach ($NCR_{C_{TK}Env}$ equal to 0.98). Also for comparison with IFM, in spectrum of the Combined Teager-Kaiser Envelope contribution of noise was higher ($NCR_{C_{TK}Env}$ equal to 0.95).

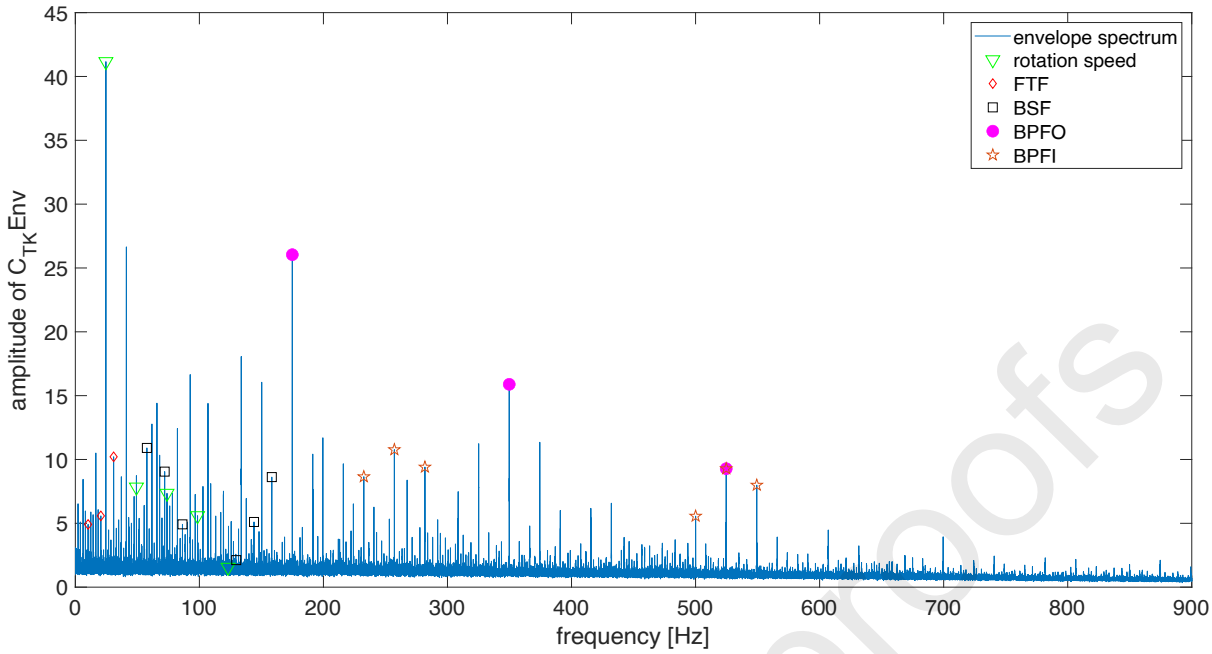

Fig. 13. Bearing OR(SF) - the $C_{TK}Env$ and the outer race fault frequency pattern indicated by the circle symbol.

3.2 Validation Case 2 – Dataset of Politecnico di Torino – Variable operating conditions

The second data set has been provided by the Department of Mechanical and Aerospace Engineering of Politecnico di Torino [48]. The set contains vibration signals recorded on a high-speed bearing operating under variable speed and load conditions. The validation process is performed using the radial vibration signals, captured on the housing of the faulty bearing.

3.2.1 Case 2 dataset description

The test stand of the Department of Mechanical and Aerospace Engineering is presented at Fig. 14. It consists of three bearings mounted on one shaft. The tested high-speed bearing is indicated as B1. The test stand is equipped with a high-speed spindle motor and a precision sledge applying radial load on the supporting bearing. The test stand has no tachometer or other speed sensor; as a result the real speed of the shaft is not measured and must be identified e.g. from the spectrum. The identified speed of the shaft during the measurements is lower than the nominal and the deviation increases with the amount of load applied on the bearing. The load is applied in the radial direction and its value is measured by a static load cell. Although, the test stand is equipped with two triaxial accelerometers, for the validation of $C_{TK}Env$, only the radial vibrations from sensor A1 are used. The data set contains signals, recorded with sampling frequency equal to 51200 Hz, from an undamaged bearing and bearings with artificially introduced defects. The faults were located on a roller and were created using a drilling process with diameter ϕ_{fail} equal to 450; 250 and 150 µm. The bearings were tested under nominal speeds of: 100, 200, 300, 400 and 500 revolutions per second and under 4 radial load conditions: no load, 1000 N, 1400 N, 1800 N. Because not all speed / load combinations were measured, the data set contains in total 51 combinations of fault size and operation conditions.

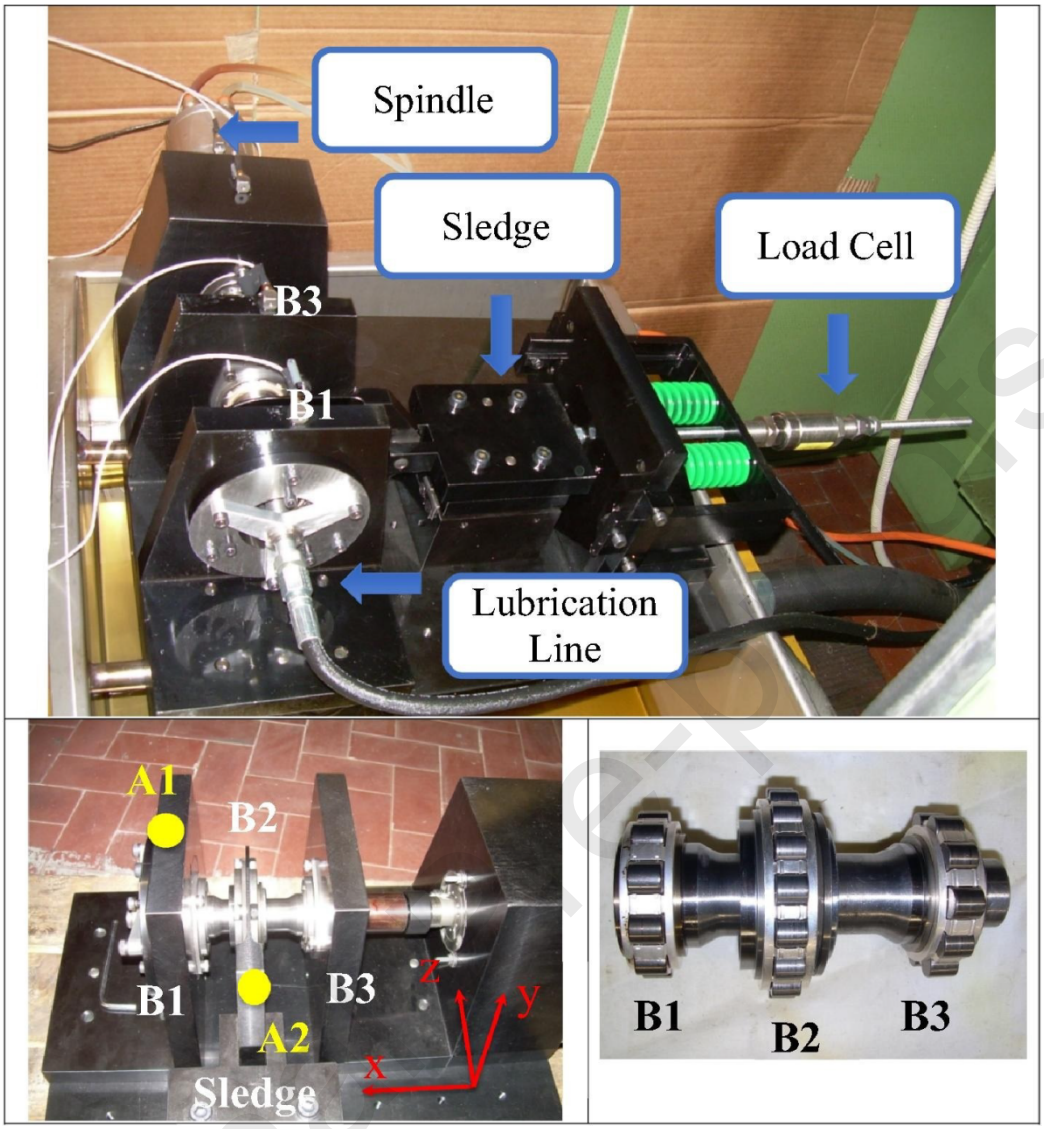

Fig. 14. The test stand of the Department of Mechanical and Aerospace Engineering: general view (up), the localization of the accelerometers A1 and A2 (bottom left), the shaft with the bearings (bottom right) [48].

The section below discusses in detail the results obtained for the 250 µm defect subset. Table 3 presents the fault characteristic frequencies for the considered case. For each rotation speed ω_{rot}, different values of the Gabor filter width were chosen. This caused the application of various numbers of filters to cover the frequency range of the analyzed signals (Table 3).

Table 3: Nominal fault frequencies for the bearing B1 for fault $\phi_{fail} = 250$ µm

Rotation speed ω_{rot} [Hz] (filter width / number of filters)	FTF [Hz]	BSF [Hz]	2xBSF [Hz]	BPFO [Hz]	BPFI [Hz]
100 (1347.5 [Hz] / 19)	38.9	213.9	427.8	388.9	611.1
200	77.8	427.8	855.6	777.8	1222.2

(2844.5 [Hz] / 9)					
300 (4266.7 [Hz] / 6)	116.7	641.6	1283.3	1166.7	1833.3
400 (6400 [Hz] / 4)	155.6	855.5	1711.1	1555.6	2444.4
500 (8533.5 [Hz] / 3)	194.4	1069.5	2138.9	1944.4	3055.6

3.2.2 Positive case example, bearing B1, $\phi_{fail} = 250$ μm, speed 400 Hz, load 1400 N

Similarly, to the first validation case, the proposed approach improved the visibility of the fault components and allowed for the identification of the fault frequencies. With respect to the noise, the $C_{TK}Env$ enhanced readability of the spectrum peaks of the fault characteristic frequencies in 31 out of 51 validation cases, compared to the result obtained using the Kurtogram. However, comparing with results obtained using EMD method, the $C_{TK}Env$ method gave better results in 46 cases from 51. The Fig. 15 and 16 present an examples of the improvement achieved using the Combined Teager-Kaiser envelope comparing to Kurtogram and EMD reference methods. The example was obtained for a rotation speed of 400 Hz and a load of 1400 N. The first and the second harmonic of the BSF modulated by the FTF, creating the classical fault pattern, can be easy identified in the $C_{TK}Env$ spectrum (Fig. 17). The $NCR_{C_{TK}Env}$ indicator (17), calculated for a frequency band, excluding the modulation peaks, i.e. $(BSF - FTF, BSF + FTF)$, was equal to 1.08 (for Kurtogram) and 3.15 (for EMD), revealing the noise suppressing capabilities of the Combined Teager-Kaiser Envelope.

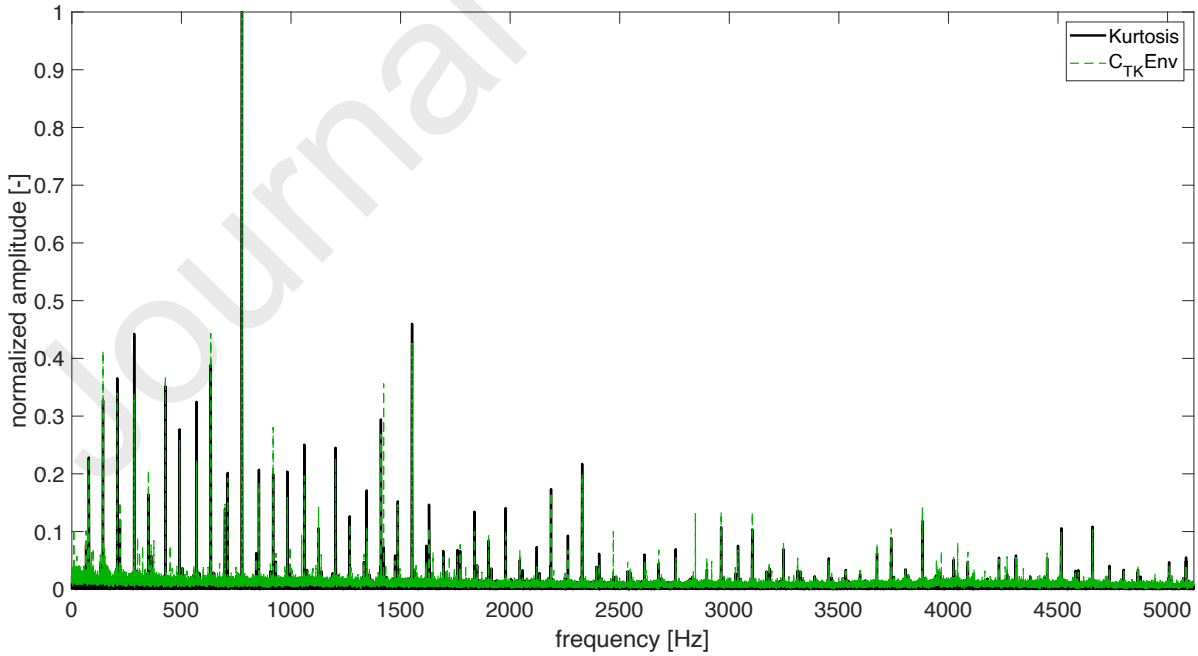

Fig. 15. Bearing B1, $\phi_{fail} = 250$ μm, speed 400 Hz, load 1400 N – comparison of the normalized $C_{TK}Env$ (green) and the normalized envelope spectrum obtained from the Kurtogram (black).

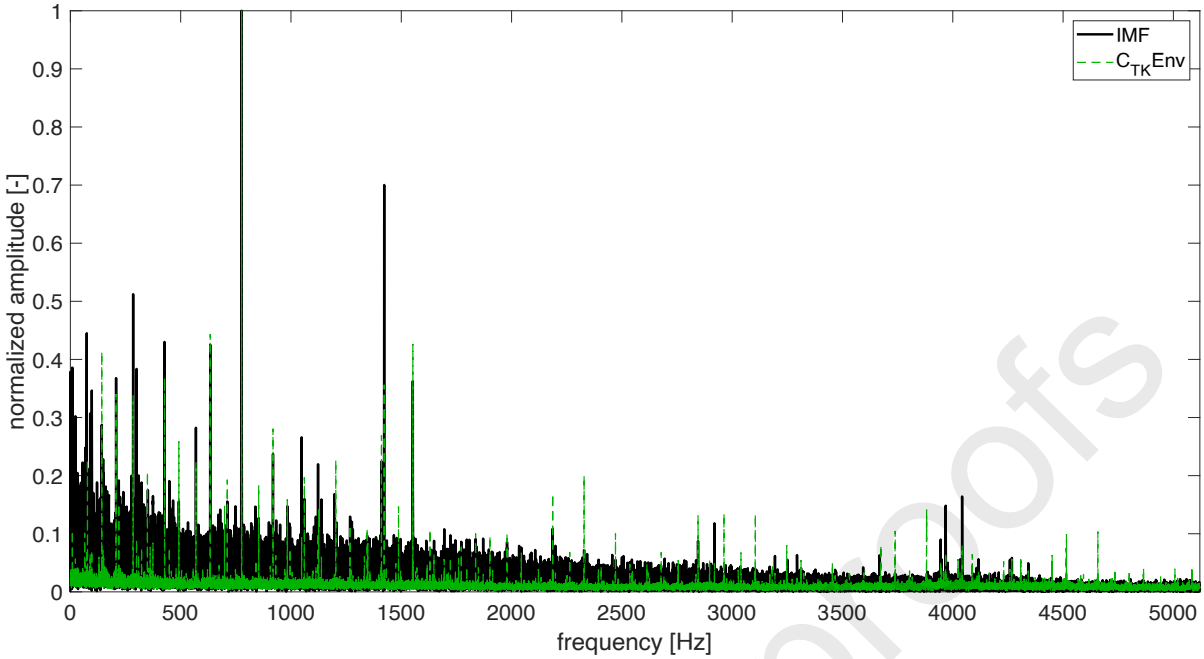

Fig. 16. Bearing B1, $\phi_{fail} = 250$ μm, speed 400 Hz, load 1400 N – comparison of the normalized $C_{TK}Env$ (green) and the normalized envelope spectrum obtained from the IMF (black).

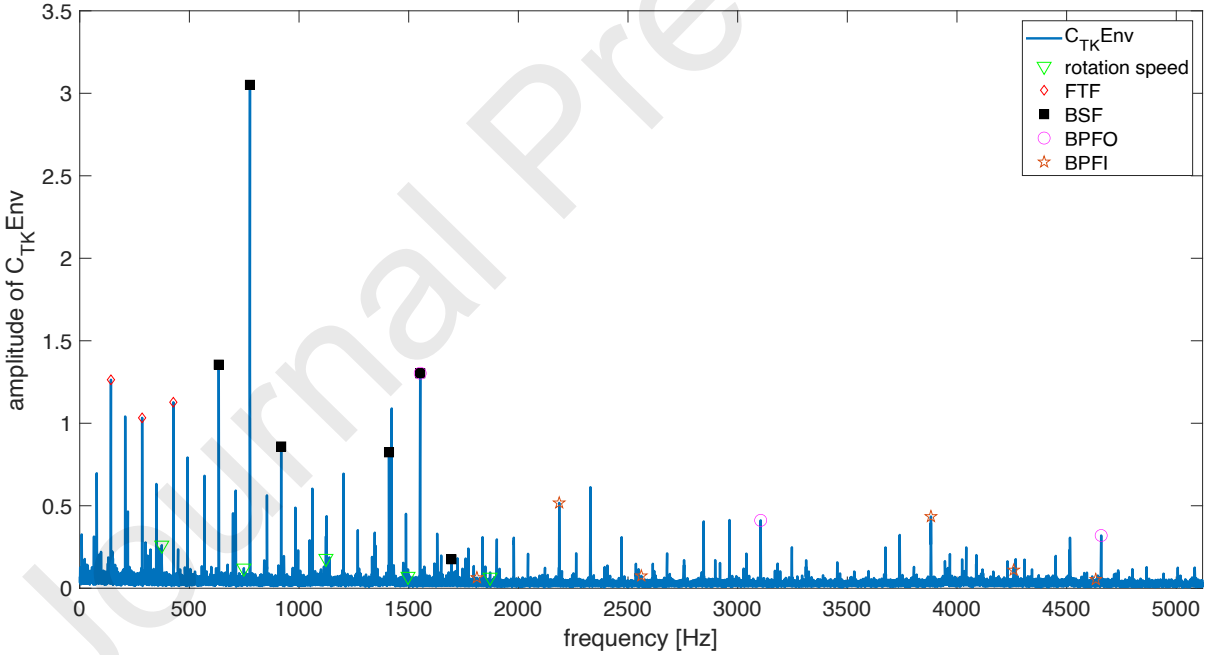

Figure 17. Bearing B1, $\phi_{fail} = 250$ μm, speed 400 Hz, load 1400 N – $C_{TK}Env$ with indicated fault characteristic components.

3.2.3 Negative case, bearing B1, $\phi_{fail} = 250$ μm, speed 300 Hz, load 1400 N

For the majority of the cases the $C_{TK}Env$ spectrum allowed obtaining better SNR comparing with the results obtained by the Kurtogram. However, for few operation conditions, such like rotation speed 300 Hz and load 1400 N or rotation speed 400 Hz and load 1000 N, the Kurtogram contained weaker noise. In this study,

those cases are considered as negative validation cases, because the $NCR_{C_{TK}Env}$ indicator, calculated for the frequency band centred around the first BSF, $(BSF - FTF, BSF + FTF)$, has value less than 1.

The Fig. 18 presents a comparison of the $C_{TK}Env$ spectrum and the spectrum of the Kurtogram for the first case mentioned above. The $NCR_{C_{TK}Env}$ indicator (17), calculated for the frequency band of interest, was equal to 0.72. The Kurtogram identified the optimal band as one defined by $fc = 14400$ [Hz] and $bw = 3200$ [Hz]. The spectrum of the Combined Teager-Kaiser Envelop contains higher noise components in the region of comparison.. However, for this case $C_{TK}Env$ gave better comparing to selected IMF ($NCR_{C_{TK}Env} = 1.02$).

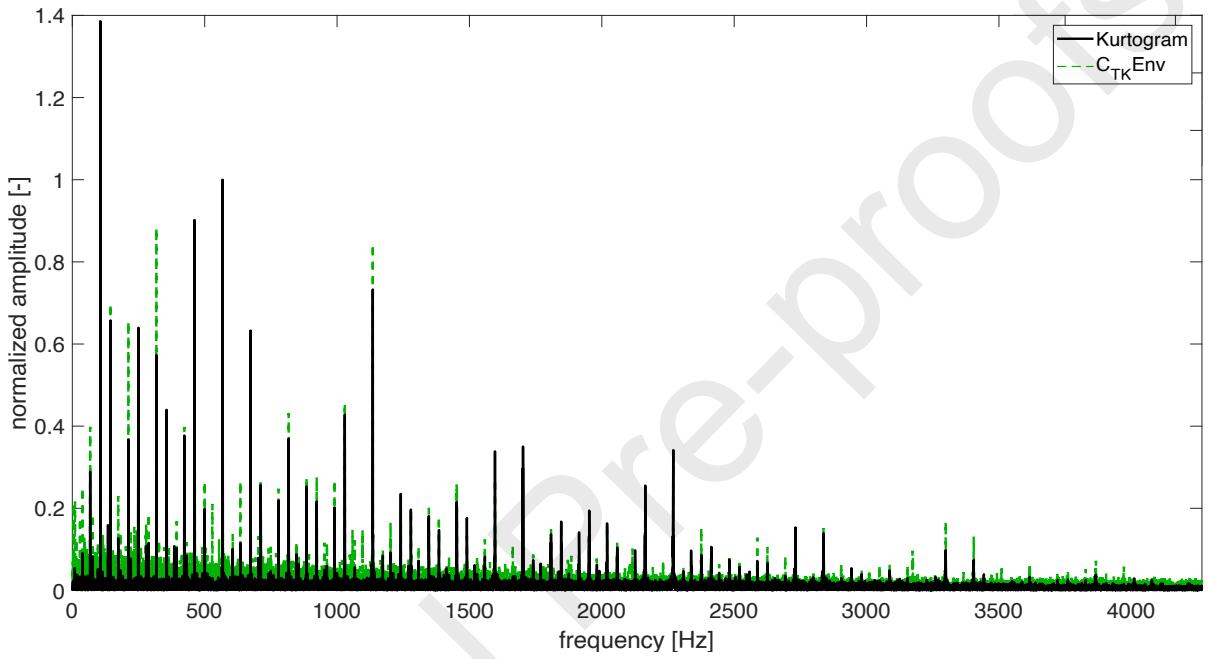

Fig. 18. Bearing B1, $\phi_{fail} = 250$ μm, speed 300 Hz, load 1400 N – comparison of the normalized $C_{TK}Env$ (green) and the normalized envelope spectrum obtained from the Kurtogram (black).

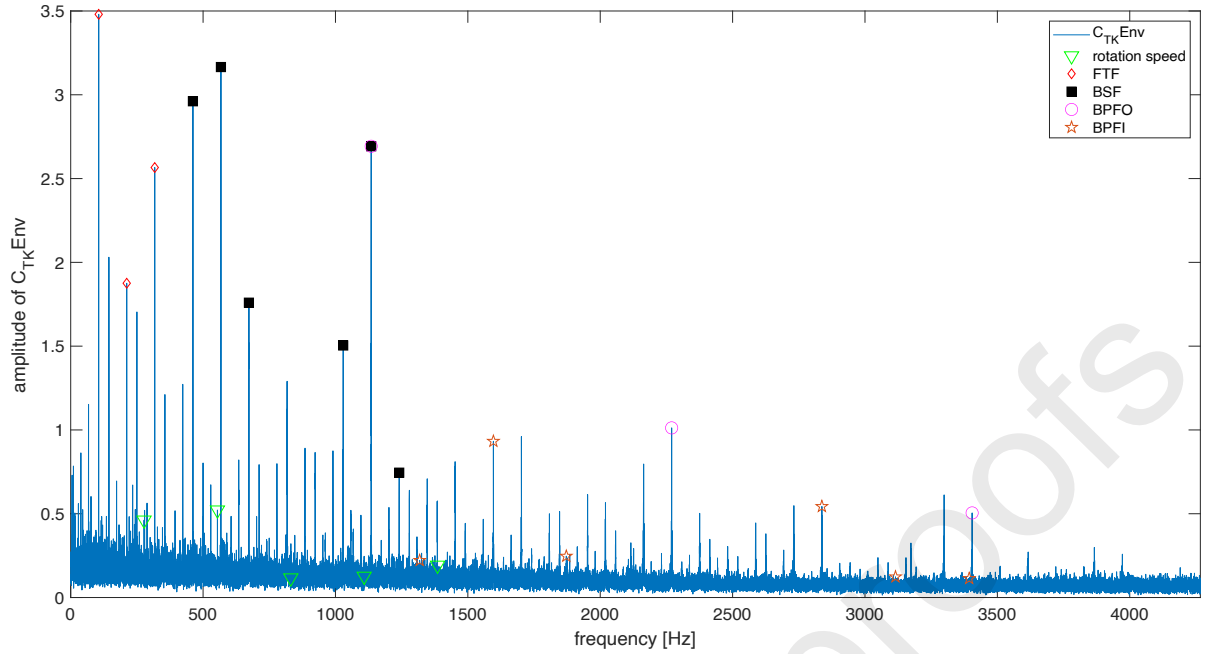

Figure 19. Bearing B1, $\phi_{fail} = 250$ μm, speed 300 Hz, load 1400 N – $C_{TK}Env$ with indicated fault characteristic components.

The result obtained for a rotation speed 400 Hz and a load of 1000 N is presented in Fig. 20. Also in this case the quality of the obtained spectrum is similar to the one obtained from the Kurtogram's most informative band $fc = 19200$ [Hz] and $bw = 12800$ [Hz]. The $NCR_{C_{TK}Env}$ indicator, calculated for a frequency band centred around the first BSF, $(BSF - FTF, BSF + FTF)$, was equal to 0.91, indicating that the contribution of the noise components is higher for the $C_{TK}Env$. Nevertheless, the set of the spectral components indicating the fault is well visible in $C_{TK}Env$ allowing for fault identification. Also for this case the IMF's noise contribution ratio slightly was grater then 1.

Analysis of other negative validation cases, i.e. the ones for which the $NCR_{C_{TK}Env} < 1$, revealed the existence of strong noise in all bands taken into account while calculating the $C_{TK}Env$ as a source of the problem. No such case was identified for which both reference methods would have smaller contribution of noise.

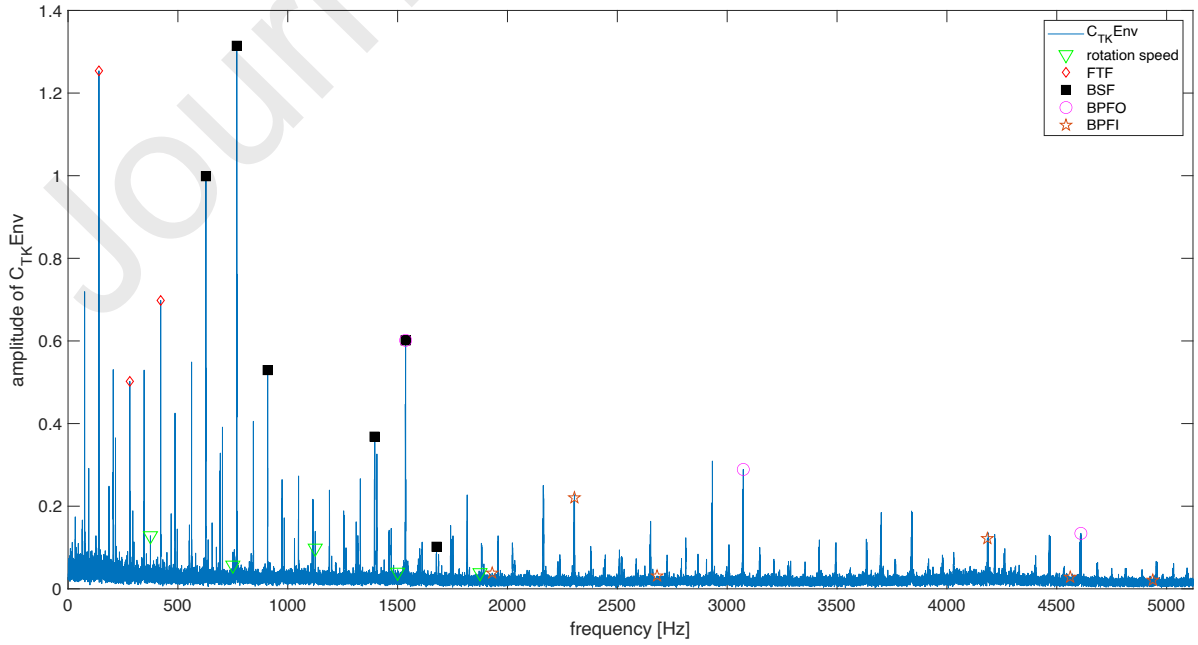

Fig. 16. Bearing B1, $\phi_{fail} = 250$ μm, speed 400 Hz, load 1000 N – $C_{TK}Env$ with indicated fault characteristic components.

4 Discussion and conclusions

In this paper the Combined Teager-Kaiser Envelope dedicated to the analysis of bearing vibration signals has been proposed. In the framework of the presented research work:

1. A novel signal processing method has been developed allowing for the enhancement of bearing fault characteristic frequencies.
2. The proposed $C_{TK}Env$ has been validated using two data sets containing signals of various faults and operation conditions.
3. The methodology achieves promising results and in the frames of this work has been compared with the state of the art methods, the Fast Kurtogram and EMD.

The application of the Teager-Kaiser Energy Operator for signal processing allows to perform a demodulation process as well as to calculate its overall energy. Presented in the paper the Combined Teager-Kaiser Envelope exploits both approaches. The envelopes obtained from bandpass filtered signals contribute to the Combined Teager-Kaiser Envelope with regard to the ratio of the bandpass signals energy to the energy of the raw signal. In this paper the method is compared with results obtained using the Kurtogram and obtained from selected IMF. The evaluation of the methods is performed using the $NCR_{C_{TK}Env}$ indicator, which has been described in the paper. This parameter allows for the comparison of the contribution of noise components in the analysed band in relation to the frequency of interest.

The $C_{TK}Env$ reveals high potential for enhancing the bearing fault frequencies and for suppressing noise components, allowing for the easier identification of the characteristic fault frequencies. The method is based on combining the diagnostic information from different frequency bands. The validation process performed on two data sets allow for the verification of the proposed approach but also for the identification of shortcomings.

In the case of the first data set, the $C_{TK}Env$ approach allowed for enhancing the frequency components testifying about the existence of the fault. The method allowed for the correct identification of the local and shallow damage of the outer race generated by sandblasting. Such fault usually results in a very weak disturbance of the signal. Similar results were obtained for other measurements from the data set. However, the $C_{TK}Env$ gave unclear results, in the cases where the fault covered the complete perimeter of the outer race, i.e. OR(SF) and OR(EF). Due to the severity of the fault, strong frequency components characteristic for other types of faults are visible in the $C_{TK}Env$, as well as strong noise contaminates all bands of filtration. This data set allowed for the validation of the method for various types of faults.

The method was also tested using another data set containing vibration signals from a high-speed bearing operating under variable speed and load. The publication discussed the measurements recorded for artificially generated faults with a diameter of 250 µm. The performed tests demonstrate the ability to enhance the diagnostically useful information for different speeds and load conditions. The faults introduced by drilling do not reflect perfectly faults arising during normal wear and the sharp edges could increase the measurement noise. Additionally, for 60,8% of the analysed cases, the results obtained by the Combined Teager-Kaiser Envelope contained lower noise components comparing to the ones based on the Kurtogram. For lest then 10% of considered cases, the IMFs'spectrums contained less noise then presented method. The $C_{TK}Env$ proved its capabilities to suppress the noise influence and to highlight the fault characteristic patterns.

The main findings of the conducted research can be summarized as:

- The use of the diagnostic information obtained from several bands of signal allows for the enhancement of the diagnostic information; such approach allowed for the development of the Combined Teager-Kaiser Envelope;

- Comparing to the Kurtogram and EMD methods, in the majority of cases, the Combined Teager-Kaiser Envelope allowed for suppressing noise components giving opportunity for easier identification of fault frequencies;
- The method is suitable for analysis of various types of bearing faults and can be applied for processing of signals recorded in various operational conditions.

The main shortcomings identified during the presented research are: the method requires the user to define the width of the Gabor filter which can influence the ability to grasp the given types of faults; the $C_{TK}Env$ method, in the present state, requires further development directed towards computation performance improvement. At present the used algorithm is approximately 2 times slower than the computationally optimized Fast Kurtogram algorithm. Although, it proved to be faster than applied EMD approach.

The presented results were obtained using data sets which contained one sample for each considered fault. Although the length of each signal was sufficient to artificially divide it into a set of diagnostic samples, the differentiation of data within a set would be neglectable and would not introduce any useful information regarding the method's performance. A new measurement campaign is planed aiming to record diagnostic signals from bigger set of bearings operating in variable operational conditions. This will allow to create an informative diagnostic data set and perform detail tests of the performance of the $C_{TK}Env$.

Although the Combined Teager-Kaiser Envelope proved its usability further improvement should be undertaken. The main direction of the future work will be the development of a fault indicator based on the $C_{TK}Env$ and the attempt to perform automatic condition identification based on the energetic contribution of the given fault patterns in the Combined Teager-Kaiser Envelope.

Acknowledgements

The authors would like to thank Ali Moshrefzadeh and Alessandro Fasana for sharing the high-speed roller bearing data and Roman Barczewski and Bartosz Jakubek for sharing the data set of the tapered roller bearing CBK-171.

A. Gałęzia gratefully acknowledged the support of the Polish National Agency for Academic Exchange granted through the project PPN/BEK/2018/1/00468/U/00001 in framework of the Bekker programme.

References

[1] S. Schmidt, P. Heyns and K. Gryllias, "A discrepancy analysis methodology for rolling element bearing diagnostics under variable speed conditions," *Mechanical Systems and Signal Processing,* vol. 116, pp. 40-61, 2019.

[2] A. Mauricio, W. A. Smith, R. B. Randall, J. Antoni and K. Gryllias, "Improved Envelope Spectrum via Feature Optimisation-gram (IESFOgram): A novel tool for rolling element bearing diagnostics under non-stationary operating conditions," *Mechanical Systems and Signal Processing,* vol. 144, 2020.

[3] A. Gałęzia, R. Barczewski and B. Jakubek, "Possibilities of Faults Detection of Rolling Bearings Using Energetic Descriptors of Vibrations Signals," in *Advances in Condition Monitoring of Machinery in Non-Stationary Operations*, 2018.

[4] Y. Lei, Intelligent Fault Diagnosis and Remaining Useful Life Prediction of Rotating Machinery, Butterworth-Heinemann, 2016.

[5] Z. Yisheng, L. Yongzhi, J. Deng, Y. Jiang and Z. Weihua, "A novel transfer learning method for bearing fault diagnosis under different working conditions," *Measurement,* vol. 171, p. 108767, 2021.

[6] A. S. Minhas, G. Singh, J. Singh, P. Kankar and S. Singh, "A novel method to classify bearing faults by integrating standard deviation to refined composite multi-scale fuzzy entropy," *Measurement,* vol. 154, p. 107441, 2020.

[7] A. Glowacz, W. Glowacz, J. Kozik, K. Piech, M. Gutten, W. Caesarendra, H. Liu, F. Brumercik, M. Irfan and Z. F. Khan, "Detection of Deterioration of Three-phase Induction Motor using Vibration Signals," *MEASUREMENT SCIENCE REVIEW,* vol. 19, no. 6, pp. 241-249, 2019.

[8] A. Głowacz, "Recognition of Acoustic Signals of Loaded Synchronous MotorUsing FFT, MSAF-5 and LSVM," *Archives of Acoustic,* vol. 40, no. 2, p. 197–203, 2015.

[9] N. Baydar and A. Ball, "A comparative study of acoustic and vibration signals in detection of gear failures using Wigner–Ville distribution," *Mechanical Systems and Signal Processing,* vol. 15, no. 6, pp. 1091-1107, 2001.

[10] G. Li, G. Tang, H. Wang and Y. Wang, "Blind source separation of composite bearing vibration signals with low-rank and sparse decomposition," *Measurement,* pp. 323-334, 2019.

[11] P. Tse, S. Gontarz and X. Wang, "Enhanced eigenvector algorithm for recovering multiple sources of vibration signals in machine fault diagnosis," *Mechanical Systems and Signal Processing,* vol. 21, no. 7, pp. 2794-2813, 2007.

[12] W. Xiong, Q. He and Z. Peng, "Fibonacci array-based focused acoustic camera for estimating multiple moving sound sources," *Journal of Sound and Vibration,* vol. 478, no. 21, p. 115351, 2020.

[13] T. Williams, X. Ribadeneira, S. Billington and T. Kurfess, "Rolling element bearing diagnostics in run-to-failure lifetime testing.," *Mechanical Systems and Signal Processing,* vol. 15, no. 5, p. 979–993, 2011.

[14] F. Xi, Q. Qiao Sun and G. Krishnappa, "Bearing diagnostics based on pattern recognition of statistical parameters," *Journal of Vibration and Control,* vol. 6, no. 3, pp. 375-392, 2000.

[15] C. Tianyou, W. Zhihua, Y. Xiang and J. Kun, "A deep capsule neural network with stochastic delta rule for bearing fault diagnosis on raw vibration signals," *Measurement,* vol. 148, 2019.

[16] R. B. Randall and J. Antoni, "Rolling element bearing diagnostics—A tutorial," *Mechanical Systems and Signal Processing,* vol. 25, no. 2, p. 485–520, 2010.

[17] M. Feldman, Hilbert transform applications in mechanical vibration, John Wiley and Sons, 2011.

[18] J. Antoni, "Fast computation of the kurtogram for the detection of transient faults," *Mechanical Systems and Signal Processing,* vol. 21, pp. 108-124, 2007.

[19] A. Moshrefzadeh and A. Fasana, "The Autogram: An effective approach for selecting optimal demodulation band in rolling element bearings diagnosis," *Mechanical Systems and Signal Processing,* pp. 294-318, 2017.

[20] P. H. Rodriguez, J. B. Alonso, M. A. Ferrer and C. M. Travieso, "Application of the Teager–Kaiser energy operator in bearing fault diagnosis," *ISA Transactions,* no. 52, p. 278–284, 2013.

[21] X. Bo, F. Zhou, H. Li, B. Yan and Y. Liu, "Early fault feature extraction of bearings based on Teager energy operator and optimal VMD," *ISA Transactions,* no. 86, pp. 249-265, 2019.

[22] A. Mauricio and K. Gryllias, "Cyclostationary-based Multiband Envelope Spectra Extraction for bearing diagnostics: The Combined Improved Envelope Spectrum," *Mechanical Systems and Signal Processing,,* vol. 149, 2021.

[23] A. Potamianos and P. Maragos, "Speech formant frequency and bandwidth tracking using multiband energy demodulation," *The Journal of the Acoustical Society of America,* vol. 99, no. 6, pp. 3795-3806, 1996.

[24] J. Kaiser, "On a Simple Algorithm to Calculate the 'Energy' of a Signal," in *Proceedings of IEEE International Conference on Acoustics, Speech, and Signal Processing*, Albuquerque, NM, 1990.

[25] G. Evangelopoulos and P. Maragos, "Multiband Modulation Energy Tracking for Noisy Speech Detection," *IEEE Transactions on Audio, Speech and Language Processing,* vol. 14, no. 16, 2006.

[26] P. Maragos and A. Potamianos, "Higher order differential energy operators," *IEEE Signal Processing Letters,* vol. vol. 2, no. No. 8, 1995.

[27] J. Kaiser, "On Teager's Energy Algorithm and its generalization to continuous signals - a simple algorithm to calculate the 'energy' of a signal," in *Proc. IEEE Digital Signal Processing Workshop*, New Paltz, NY, 1990.

[28] E. Kvedalen, Signal processing using the Teager Energy Operator and other nonlinear operators, Cand. Scient Thesis, University of Oslo, Department of Informatics, 2003.

[29] K. Gryllias and I. Antoniadis, "Application of the Energy Operator Separation Algorithm (EOSA) for the instantaneous amplitude and frequency calculation of nonlinear dynamic systems response," in *DETC2009-87375, Proceedings of the ASME 2009 International Design Engineering Technical Conferences & Computers and Information in Engineering Conference, IDETC/CIE 2009,*, San Diego, California, USA, 2009.

[30] A. Gałęzia and A. Orłowska-Gałęzia, "Application of Teager–Kaiser's Instantaneous Frequency for Detection of Delamination in FRP Composite Materials," *Materials,* no. 14(5), 1154;, pp. 1-24, 2021.

[31] I. Antoniadou, T. Howard, R. Dwyer-Joyce, M. Marshall, J. Naumann, N. Dervilis and K. Worden, "Envelope Analysis Using the Teager-Kaiser Energy Operator for Condition Monitoring of a Wind Turbine Bearing," *Applied Mechanics and Materials,* vol. vol. 564, pp. 170-175, 2014.

[32] R. B. Randall and W. A. Smith, "Uses and mis-uses of energy operators for machine diagnostics," *Mechanical Systems and Signal Processing,* vol. 133, 2019.

[33] R. Gu, J. Chen, R. Hong, H. Wang and W. Wu, "Incipient fault diagnosis of rolling bearings based on adaptive variational mode decomposition and Teager energy operator," *Measurement,* vol. 149, p. 106941, 2020.

[34] A. Gałęzia, "Teager-Kaiser energetic trajectory for machine diagnosis purposes," *Journal of Vibroengineering,* vol. vol. 19, no. no. 2, p. 1014–1025, 2017.

[35] T. Han, Q. Liu, L. Zhang and A. C. Tan, "Fault feature extraction of low speed roller bearing based on Teager energy operator and CEEMD," *Measurement,* vol. 138, pp. 400-408, 2019.

[36] M. Liang and B. Soltani, "An energy operator approach to joint application of amplitude and frequency-demodulation for bearing fault detection," *Mechanical Systems and Signal Processing,* vol. Vol. 24, p. 1473–1494, 2010.

[37] P. Maragos, J. Kaiser and T. Quatieri, "On Amplitude and Frequency Demodulation Using Energy Operators," *IEEE Transactions on Signal Processing,* vol. vol. 41, pp. 1532-1550, 1993.

[38] D. Dimitriadis and P. Maragos, "An improved energy demodulation algorithm using splines," in *Acoustics, Speech, and Signal Processing, 2001. Proceedings. (ICASSP '01). 2001 IEEE International Conference onVolume: 6*, 2001.

[39] D. Gabor, "Theory of communication," *Journal of the Institution of Electrical Engineers,* vol. 93, pp. 429-441, 1946.

[40] N. E. Huang, Z. Shen, S. R. Long, M. C. Wu, H. H. Shih, Q. Zheng, N.-C. Yen, C. C. Tung and L. H. H., "The Empirical Mode Decomposition and the Hilbert Spectrum for Nonlinear and Non-Stationary Time Series Analysis," *Proceedings of the Royal Society of London. Series A: Mathematical, Physical and Engineering Sciences,* p. 903–995, 1998.

[41] X. Zhang, Y. Liang, J. Zhou and Y. Zang, "A novel bearing fault diagnosis model integrated permutation entropy, ensemble empirical mode decomposition and optimized SVM," *Measurement,* vol. 69, pp. 164-179, 2015.

[42] Y. Zhang, J. Ji and B. Ma, "Fault diagnosis of reciprocating compressor using a novel ensemble empirical mode decomposition-convolutional deep belief network," *Measurement,* vol. 156, p. 107619, 2020.

[43] J. Zheng, M. Su, W. Ying, J. Tong and Z. Pan, "Improved uniform phase empirical mode decomposition and its application in machinery fault diagnosis," *Measurement,* vol. 179, p. 109425, 2021.

[44] P. Flandrin, R. G. and P. Goncalves, "Empirical mode decomposition as a filter bank," *IEEE Signal Processing Letters,* vol. 11, no. 2, pp. 112-114, 2004.

[45] P. Flandrin, P. Gonçalvès and G. Rilling, "Detrending and denoising with empirical mode decompositions," in *12th European Signal Processing Conference (EUSIPCO 2004)*, Vienna, Austria, 2004, September 6-10,.

[46] A. Boudraa and J. Cexus, "EMD-Based Signal Filtering," *IEEE Transactions on Instrumentation and Measurement,* vol. 56, no. 6, pp. 2196-2202, 2007.

[47] J. Dybała and R. Zimroz, "Rolling bearing diagnosing method based on Empirical Mode Decomposition of machine vibration signal," *Applied Acoustics,* vol. 77, 2007.

[48] A. Daga, A. Fasana, S. Marchesiello and L. Garibaldi, "The Politecnico di Torino rolling bearing test rig: Description and analysis of open access data," *Mechanical Systems and Signal Processing,* no. 120, pp. 252-273, April 2019.

Credit Author Statement

Manuscript title: Application of the Combined Teager-Kaiser Envelope for bearing fault diagnosis

Authors contribution:

Adam Gałęzia: Methodology, Software, Validation, Formal analysis, Investigation, Writing - Original Draft, Visualization

Konstantionos Gryllias: Conceptualization, Resources, Writing - Review & Editing,

Declaration of interests

☐ The authors declare that they have no known competing financial interests or personal relationships that could have appeared to influence the work reported in this paper.

☒The authors declare the following financial interests/personal relationships which may be considered as potential competing interests:

Polish National Agency for Academic Exchange granted Adam Galezia through the project PPN/BEK/2018/1/00468/U/00001 in framework of the Bekker programme.